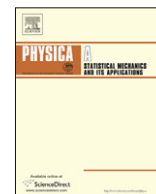




Contents lists available at ScienceDirect

Physica A

journal homepage: www.elsevier.com/locate/physa

Topological efficiency in three-dimensional gallery networks of termite nests

Andrea Perna^{a,b,*}, Sergi Valverde^{a,c}, Jacques Gautrais^{a,b}, Christian Jost^a, Ricard Solé^c, Pascale Kuntz^b, Guy Theraulaz^a

^a Centre de Recherches sur la Cognition Animale, CNRS UMR 5169, Université Paul Sabatier, 118 route de Narbonne, 31062 Toulouse Cedex 4, France

^b Laboratoire d'Informatique de Nantes Atlantique, Site Ecole Polytechnique de l'Université de Nantes, La Chantrerie, BP50609, 44306 Nantes Cedex 3, France

^c ICREA-Complex Systems Lab, Universitat Pompeu Fabra, Dr. Aiguader 80, 08003 Barcelona, Spain

ARTICLE INFO

Article history:

Received 22 March 2008

Received in revised form 3 July 2008

Available online xxxx

Keywords:

Spatial networks

Social insects

Transportation networks

Self organized structures

ABSTRACT

Transport networks are a key component of human and natural societies that enable efficient communication at a low cost. Here, we study the topological efficiency of the three-dimensional networks of galleries in termite nests and how spatial constraints affect the organisation of these networks. *Cubitermes* termite nests have far better than random transportation efficiency, but they do not reach theoretical optimal performance. We rather suggest a multiobjective process where a number of additional requirements, such as resilience to external attacks and the presence of spatial constraints, limit the ability of the system to achieve maximal transportation performance.

© 2008 Elsevier B.V. All rights reserved.

1. Introduction

Animals and humans move across the space following preferential paths. These are the trails, tracks, roads, rails and air routes that compose large transportation networks.

In human built transportation networks, planning and design take an active part in shaping the final network topology. On the contrary, animal built networks grow out of the merging and intersection of individual paths formed by individuals that in general do not possess a global knowledge of the whole structure. For this reason animal transportation networks are particularly interesting, because they are completely self-organised [1].

Transportation networks are spatial networks, that is, networks where the probability for two vertices to be connected is function of their relative distance [2] (see also Ref. [3] for review). Spatial planar networks have received much attention in recent literature because of their capability to describe human transportation systems and street patterns [4–9]. Human built transportation networks, sometimes deviate from planarity in the sense that vertices all lie on a 2-dimensional plane, but edges are not constrained to connect to spatial “neighbours”. This is the case, for instance, of the world-wide air transportation network [10,11], the physical internet wiring [12], or wireless networks.

In order to understand the properties of a particular real world transportation network, papers typically compute many network estimators. On the theoretical ground they usually address the question ‘what is the optimal transportation network given a set of constraints and a particular objective of optimisation?’. Comparing the properties of the real world networks with the “optimal” network model, it is possible to make hypotheses about which factors have shaped the real network topology.

* Corresponding author at: Centre de Recherches sur la Cognition Animale, CNRS UMR 5169, Université Paul Sabatier, 118 route de Narbonne, 31062 Toulouse Cedex 4, France. Tel.: +33 6 28806636.

E-mail address: perna@cict.fr (A. Perna).

Typical examples of optimal networks include *minimum spanning trees* (MST, the network that connects all the vertices at the minimum total cost), *shortest path spanning trees* (the spanning trees with minimum distance between its root and any other vertex), and spanning trees minimising the average or maximum distance between all pairs of vertices (respectively the *minimum average stretch spanning tree* MAST and the *minimum maximum stretch spanning tree* MMST). Usually, however, complex real world networks grow under the effect of multiple forces and multiple constraints. In order to evaluate the performance of these networks, more complex optimality criteria have been considered.

In general one can distinguish between rooted transportation networks (where all the flows originate from a single source or are directed toward a single sink) and unrooted, distributed networks where resources are exchanged between many vertices. In the context of rooted networks Banavar et al. [13] study transportation networks that provide a route from a root vertex (the source) to all the L^D sites uniformly distributed in a D -dimensional space. In this context, they describe a class of efficient networks that minimise the total flow over all the edges $\sum_{e_{ij}} |I(e_{ij})|$ (where $|I(e_{ij})|$ is the magnitude of flow on the edge e_{ij}). In this model, networks can have loops. However, if no local constraint is imposed on the carrying capacity of individual edges, the optimal networks are trees [14]. Gastner and Newman [9] use a model of network generation that minimises both distance from the root and the total length of edges to simulate the properties of four real world transportation networks.

Urban street patterns are unrooted distributed networks with all vertices having similar importance. Buhl et al. [6] and Cardillo et al. [7] have studied the cost and robustness of urban streets networks comparing them with two extreme models: the Minimum Spanning Tree and the Greedy Triangulation (the planar network with the highest number of edges and low total cost).

In many cases, the relevant properties of unrooted transportation networks have been well reproduced by optimisation models that minimise an average network quantity. The exact measure to be minimised changes in different studies, but in general it basically involves a measure of distance that can be combined with additional parameters and constraints. Colizza et al. [15] study optimal networks minimising two parameters: average path length and traffic congestion (this latter assumed to be proportional to vertex degree). These authors show that a variety of networks can be generated simply varying a control parameter, so as to give more importance to either path length or congestion. Gastner and Newman [16] minimise edge “effective length”, where the “effective length” of an edge is a weighted average between its topological and Euclidean distances. The optimisation is performed under the constraint that the total cost of the network must not exceed a given value. Depending on the values of the control parameter, this model can simulate different classes of networks ranging from networks resembling urban street patterns to networks more similar to the air transportation network. In Barthelemy and Flammini [17] optimal traffic networks result from minimisation of an average cost function along all the shortest paths. The cost here is proportional to the length of the edge and inversely proportional to the traffic (it is assumed that the more traffic there is along an edge, the easier it will be to find a fast connection).

However, minimisation of an average quantity is not necessary to reproduce some characteristics of human transportation networks. For instance, Barthelemy and Flammini [18] show that some of the peculiar properties of urban street patterns are well described by a local growth model where new vertices are connected to the existing network through the cheapest connections.

Animal built transportation networks have received less attention in the literature, in part because of the lack of accurate characterisations of real world networks. Animal transportation networks have important ecological and biological functions. They favour animal orientation [19,20] and regulate interactions between individuals, communities or species [21, 22]. It is likely that the topology of such networks has been shaped by selective pressures associated to the above functions.

Most animal displacements follow paths and trails *on the ground* that are well described by planar networks. Buhl et al. [23] describe an underground system of galleries excavated by ants that is also well represented by a planar network (though here the planarity is somehow imposed by experimental constraints).

However, there exist also animal transportation networks that are 3-dimensional. One of these is the gallery system inside the nests of termites. Termites are known for building huge and extremely complex nests [24,25]. In most cases the nests do not simply result from the repetition of local patterns, but present a coherent global organisation.

The nests of African termites of the Macrotermitinae subfamily in particular have attracted much attention in the literature [26–32]. Termites of this subfamily build mounds that are up to six metres high and house millions of insects, each less than 1 cm in length. Inside the mounds, the termites accumulate plant material that they use to grow a particular genus of mushrooms (*Termitomyces*), used as food by the colony. The fungi and termites together have a high metabolism, and produce abundant CO₂ and heat. Many studies have shown that the particular form of the mound and the inner air channels contribute to maintain the optimal levels of temperature and CO₂ necessary to the colony.

Phenomena such as thermoregulation and ventilation represent important examples of adaptive properties of termite nests, but they are likely to be ecologically important functions only for big colonies of fungus growing termites. Nevertheless, other aspects of nests built by all termite species are worth emphasising. In particular, we consider here the fact that inside the nests of almost all termite species are huge networks of galleries and chambers that span the three dimensions. These are one of the rare described examples of 3D transportation networks. Their topological properties are also likely to be extremely relevant for the ecology and the survival of the termite colony. In fact termites spend most of their life inside a single network, comprising the galleries inside the nest and other subterranean galleries that connect the nest to the foraging sites [25].

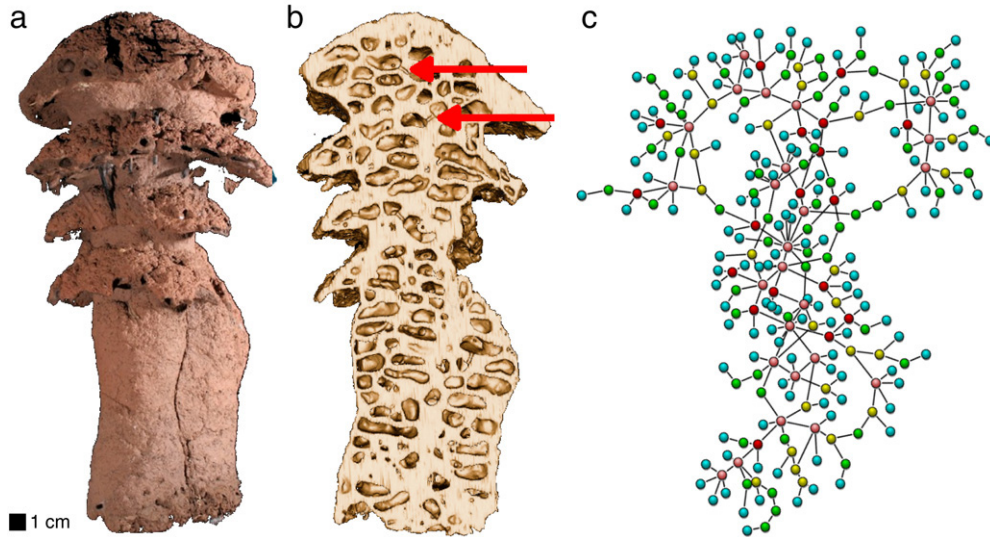


Fig. 1. Left: Picture of one nest (M11); centre: a tomographical cut of the same nest (the arrows indicate two of the corridors between chambers); right: a representation of chambers and galleries as a network, where each vertex corresponds to a chamber in the original nest and each edge to a corridor. The colour of the vertices reflects their degree; vertex positions have been adjusted to improve visibility.

3-D networks have received little attention in the literature, partly because of the added level of complexity and the difficulties of capturing and detecting the spatial patterns.

Here, we study six 3-D networks of galleries found in nests built by *Cubitermes* termites. Termites of this genus build above ground nests of relatively small size (30 cm) whose shape resembles that of a mushroom (Fig. 1.a) covered by one or more caps [25]. These nests are filled with tightly packed chambers (Fig. 1.b). Adjacent chambers can be connected by a simple opening or short corridor (two corridors are indicated by arrows in Fig. 1.b). As a general rule, no long-distance connections are possible, and chambers that are not physically adjacent are never directly linked by a corridor. In this termite genus, new chambers (network vertices) are added at the top of the nest during periods of rapid building activity, and are never rearranged [33]. On the contrary, the number and position of corridors (network edges) change across the whole nest life [34].

We measure the level of communication efficiency achieved by 3-D *Cubitermes* nests. Termite nests have far better than random transportation efficiency, but they do not reach theoretical optimal global performance. Our study suggests that the origin of this deviation stems from a multi-objective optimisation process under spatial constraints.

2. Methods

Six *Cubitermes* nests were used. The nests, labelled M9, M10, M11, M12, M18 and M19 belonged to private or public collections (Natural History Museums of Paris and Toulouse) and originated from different locations in Central African Republic and Cameroon. Nests were reconstructed into 3-D virtual volumes using X-ray tomography with a medical scanner [35]. For every nest, we obtain the transportation network $G = (V, E)$ corresponding to the biggest set of physically interconnected chambers in the original nest (Fig. 1.c). In this network, a vertex $v_i \in V$ represents a physical chamber and an edge $e_{ij} = \{v_i, v_j\} \in E$ depicts a physical corridor between chambers v_i and v_j . We can reconstruct the network G by a process of dilation, as follows. Chamber “cores” are defined as small empty regions located farther than about 1.5 mm from nest walls (internal or external). Given the narrow diameter of the corridors (less than ~ 1.0 mm) these regions either belong to a chamber or to the space outside the nest, but never to a corridor. The chamber cores were identified as the network vertices. They were then concurrently dilated to progressively fill their surrounding empty space (stopping at walls). At some point, a dilated core also crams into its outgoing corridors and gets in touch with the other dilated cores coming from the other end of the corridor. In this case, an edge between the vertices was created, corresponding to the physical corridor.

To obtain the virtual network corresponding to the case when all physically adjacent chambers would be connected (G_M ; see later), the dilation of the same chamber cores was repeated in the pure 3D-space up to the complete space filling (neglecting now the nest walls). When two dilated cores got in touch, they were marked as adjacent. The results of this automatic segmentation were verified and manually corrected. A schematic exemplification of the networks reconstruction procedure is shown in Fig. 2.

Once we have recovered the gallery network, we can compute several topological measurements. We define the degree k_i of vertex v_i as the number of edges attached to it, with $k_{\max} = \max\{k_i\}$ being the maximal degree of the network. The average degree $\langle k \rangle = \sum k_i / N$ (where N is the vertex number of G) indicates the level of network sparseness. We can also

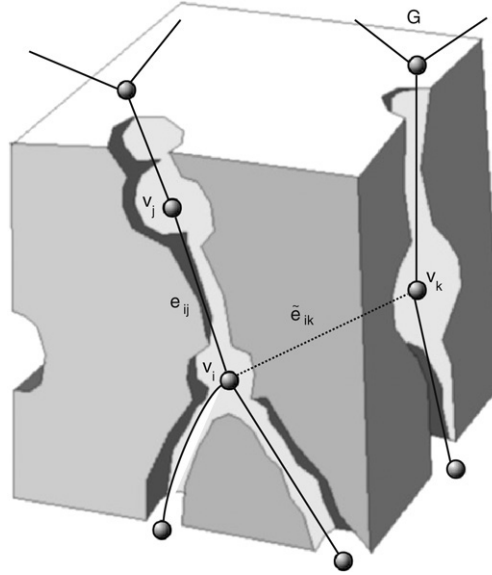


Fig. 2. Building networks from tomographic scans. Here we show a small piece of a termite nest including some chambers and corridors. Connected chambers such as v_i and v_j appear linked through an edge e_{ij} on the G graph. A different possibility is to establish an edge \tilde{e}_{ik} between two nearest chambers that are not physically linked. These cases define the G_M graph, where two close vertices do not need to be physically linked through a gallery.

measure the patterns of connections involving more than one vertex. Four important measures characterise the global nest structure. The first two are small-world measures, namely, average path length L and clustering coefficient C . Average path length L is defined as follows:

$$L = \frac{1}{N(N-1)} \sum_{v_i, v_j} d(v_i, v_j) \quad (1)$$

where $d(v_i, v_j)$ is the topological path length or the minimal number of corridors that a termite must traverse to navigate between any pair of vertices v_i and v_j . Average path length is a measure of network spread or compactness. For example, networks with low L can be efficiently navigated. In this context, L is an adequate topological measure for nest galleries because all corridors and chambers are similar in length and size.

The clustering coefficient C is defined as the probability that two vertices that are neighbours of a given vertex are also neighbours of each other (i. e. that a triangle is formed). In order to estimate C , we define for each vertex v_i a neighbourhood P_i composed of all the vertices v_j that are linked to v_i . Every vertex $v_j \in P_i$ can also be linked to each other, and the (local) clustering coefficient $C(P_i)$ is defined as follows:

$$C(P_i) = \frac{1}{k_i(k_i-1)} \sum_{v_j} \sum_{v_k \in P_i} A_{jk} \quad (2)$$

where the adjacency matrix $A_{jk} = 1$ if there is an edge between v_j and v_k or $A_{jk} = 0$ otherwise. The clustering coefficient for the whole graph is then computed as the average of $C(G) = \langle C(P_i) \rangle$.

Shortest paths enable us to define a static measure of traffic flow in networks. In this context, betweenness centrality (BC) of the element $v \in G$, either a vertex or an edge, is defined as follows:

$$BC(v) = \sum_{v_i \neq v_j} \frac{c_{ij}(v)}{c(v_i, v_j)} \quad (3)$$

where $c_{ij}(v)$ is the number of shortest paths from vertex v_i to vertex v_j passing through element v and $c(v_i, v_j)$ is the total number of shortest paths from v_i to v_j [36]. This is a topological surrogate (in many cases) of the vertex relevance in terms of flows. Vertices that occur on many shortest paths between other vertices have higher betweenness than those that do not.

We also define a measure of local graph redundancy $R(G)$, that evaluates the length of the cycles in the graph, and is calculated as follows:

$$R(G) = \frac{1}{N(N-1)} \sum_{v_i, v_j} \frac{2}{r(v_i, v_j)} \quad (4)$$

where the edge range $r(v_i, v_j)$ is the length of the shortest path from v_i to v_j in the absence of the edge e_{ij} [37,38]. This value is comprised between 0 and 1. In particular, $R(G) = 0$ for trees (where $d(v_i, v_j) = \infty$ if we remove the edge e_{ij}) and $R(G) = 1$ for graphs where every edge belongs to at least one triangle.

Table 1

Properties of the observed networks of galleries (RN) and of the maximal graph that could have been embedded in the space of the same nest (MEG)

Nest	N	$ E $	$\langle k \rangle$	k_{\max}	L	cc	Redundancy
M9-RN	507	676	2.67 ± 0.08	10	8.51	0.038	0.374
M9-MEG	507	2836	11.19 ± 0.19	25	5.76	0.495	1.000
M10-RN	349	359	2.06 ± 0.07	8	16.91	0.003	0.060
M10-MEG	349	1553	8.90 ± 0.20	21	9.43	0.539	1.000
M11-RN	260	280	2.15 ± 0.10	12	9.11	0.009	0.144
M11-MEG	260	1196	9.20 ± 0.26	24	6.22	0.533	0.996
M12-RN	183	233	2.55 ± 0.13	9	8.19	0.011	0.344
M12-MEG	183	854	9.33 ± 0.26	20	5.08	0.524	1.000
M18-RN	287	342	2.39 ± 0.10	10	8.40	0.034	0.276
M18-MEG	287	1461	10.18 ± 0.26	24	5.49	0.502	1.000
M19-RN	268	437	3.27 ± 0.14	12	7.89	0.116	0.596
M19-MEG	268	1259	9.40 ± 0.22	22	6.52	0.501	0.996

N = number of vertices; $|E|$ = number of edges; $\langle k \rangle$ = mean degree; k_{\max} = max degree; L = average topological path length; cc = clustering coefficient.

3. Results

3.1. Topological constraints imposed by spatial embedding

In our 3-D spatial network, vertices completely fill the space without any overlap or gap and thus connections are only possible between physically adjacent elements. Is the spatial arrangement of chambers and galleries somewhat optimal? More precisely, are chambers connected through galleries maximising transportation efficiency (for a given cost of edges). In order to study the possible presence of optimality in these networks, we define the *maximal embedded graph* (MEG) as the network $G_M = (V, E_M)$ with the same set of vertices as in the transportation network G but now there is a edge $\{v_i, v_j\} \in E_M$ if chambers v_i and v_j are separated by a single wall (i.e., v_i and v_j are adjacent), independently if they were also physically connected by a corridor or not.

When there are no long distance connections between non-adjacent chambers (i.e. long chains in the associated graph), a MEG contains the whole edge set allowed by the constraints of the spatial embedding. Hence, all the possible networks compatible with these constraints can be generated as subgraphs of a MEG. We here restrict ourselves to spanning subgraphs of G_M i.e. connected graphs $G = (V, E_S)$ with the same vertex set V , and an edge set $E_S \subset E_M$ subset of E_M .

The topological assumptions required by our model have been checked in the real *Cubitermes* nests. There are no long-range connections in these nests; all the connections take place between physically adjacent chambers. Otherwise stated, the edges of the real nests are a subset of G_M edges in the vast majority of the cases. These properties were verified for nests M9, M11, M12, M18 and M19; in each of these nests around 99% of the edges were also edges of G_M . The remaining about 1% of the edges connected chambers adjacent at a corner, and for this reason these edges were not marked as adjacent by the automatic segmentation procedure. We added these edges to G_M . Nest M10 displays a different behaviour because termites have built some long-range corridors on the external surface of the nest that link to distant chambers. For this reason, nest M10 was not used in some of the analyses.

Table 1 shows network measurements for the nests and their corresponding maximally embedded graph. The comparison of nest G and the G_M indicates the presence of strong constraints to the possible nest architectures. No network can have more edges than G_M :

$$|E| \leq |E_M|. \quad (5)$$

As defined, no network embedded in the same space can have higher values of $\langle k \rangle$ or k_{\max} than the associated G_M . In addition, shortest path length is directly correlated to network size and inversely correlated with connectivity. Similarly, there are upper bounds to the clustering coefficient and the graph redundancy. However, gallery networks are far from the limit defined by the maximally embedded graph because they are very sparse. That is, vertices have smaller degree than the one predicted by the spatial constraints alone.

Fig. 3 reports the degree distribution $P(k)$ in the six nests (black closed circles) and the G_M (open circles), plotted on a log-linear scale. The distribution (continuous black line) is single scaled and follows an exponential distribution:

$$P(k) \sim e^{-k/\gamma} \quad (6)$$

with $1.46 \leq \gamma \leq 2.65$ for the network dataset analysed here. Interestingly, this distribution cannot be obtained by randomly sampling the G_M network (which leads to a Poisson distribution, instead). In the following, we present a set of more appropriate models for these gallery networks.

3.2. Modeling termite nest topology

The differences between real gallery networks and corresponding maximal embedded graphs suggest that chamber proximity is not the only mechanism that shapes network topology. More restrictive factors seem to limit connectivity

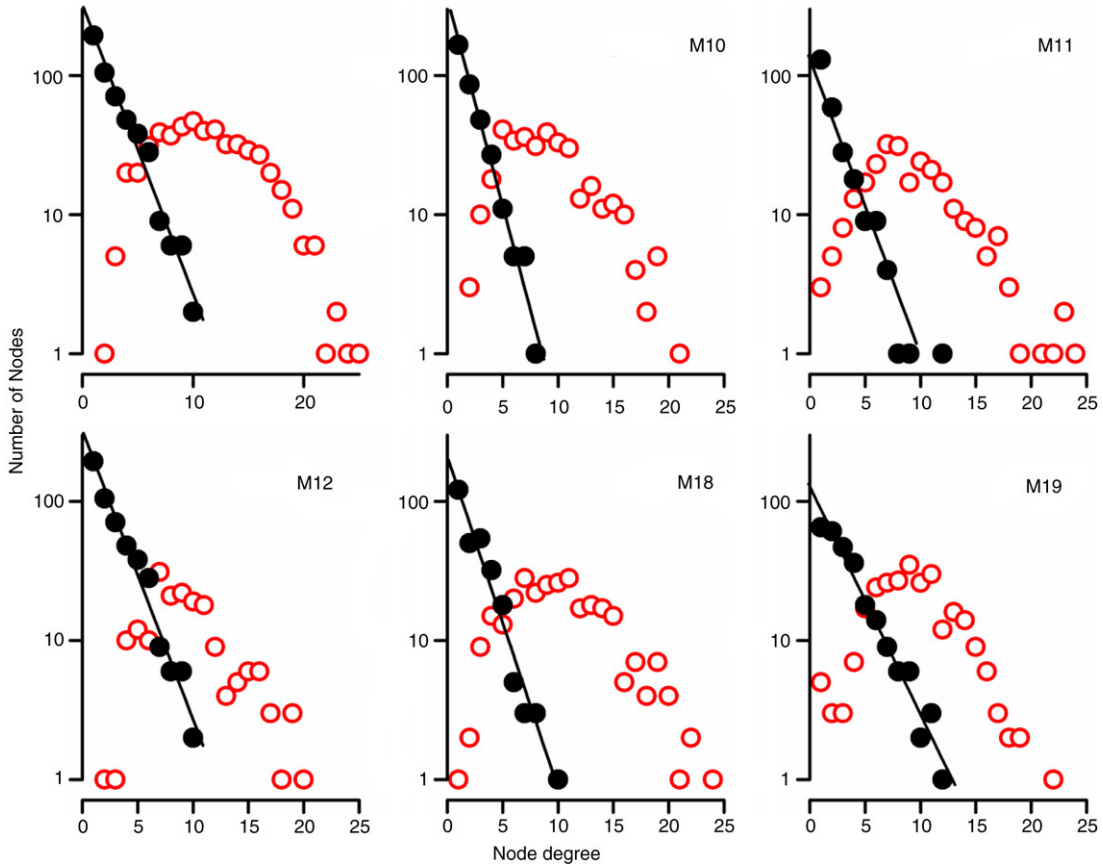


Fig. 3. Degree distribution in the gallery network G (closed black circles) and in the maximally embedded graph G_M (red open circles) for the six studied nests. The probability of a vertex having degree k is well fitted by the exponential function $P(k) \sim e^{-\frac{k}{\gamma}}$, with γ values 2.09 (nest M9), 1.46 (nest M10), 2.02 (nest M11), 2.40 (nest M12), 1.82 (nest M18), 2.65 (nest M19) (continuous black curve).

below the theoretical maximum provided by G_M . Here, we further investigate the indirect effects of spatial embedding comparing the properties of gallery networks against spatial network models. The spatial constraints are integrated in the models by imposing that these networks be spanning subgraphs of G_M . If the characteristics of the real gallery network are mainly a consequence of the spatial embedding, then spanning subgraphs of G_M with the same connectivity will also display similar features.

In the following, we compare gallery networks with two classes of spanning subgraphs of G_M : random and maximal betweenness networks.

- (1) Random spanning subgraphs: We generate these networks by first generating a random spanning tree [39] of the G_M . Then, we insert additional edges (chosen with uniform probability among the edges in G_M) until we reach the same number of edges as in the observed gallery network G .
- (2) Maximum BC spanning subgraphs: The real networks of galleries were also compared with spanning subgraphs aimed at having particularly short path lengths between all pairs of vertices. These were generated with the following algorithm. Starting from the G_M network, perform the following steps:
 - (i) compute the BC for all the G_M edges and sort the edges by increasing BC order.
 - (ii) Delete the edge in G_M with the lowest BC value if the network connection is preserved; otherwise keep the edge and go to the next one.
 - (iii) Repeat (ii) until the edge number of the resulting network and of the observed network are equal.
 In step (ii), if many edges have the same BC value, choose one at random.

The maximum BC algorithm tries to keep path lengths short by greedily preserving edges that take part in a high number of shortest paths (with high BC). This maximum BC-spanning graph is similar to the maximum centrality spanning trees (MCST) defined in [40], but here the computation of betweenness is reiterated at each step of the algorithm. This model was chosen because it is at least theoretically a plausible model for termite network evolution. First, there is empirical evidence that the real gallery networks are *not* reached by adding new elements to the network, but at least in part, by progressively removing corridors. For example, nest M19 was under construction when it was collected, and this nest has a higher number of connections than the other nests.

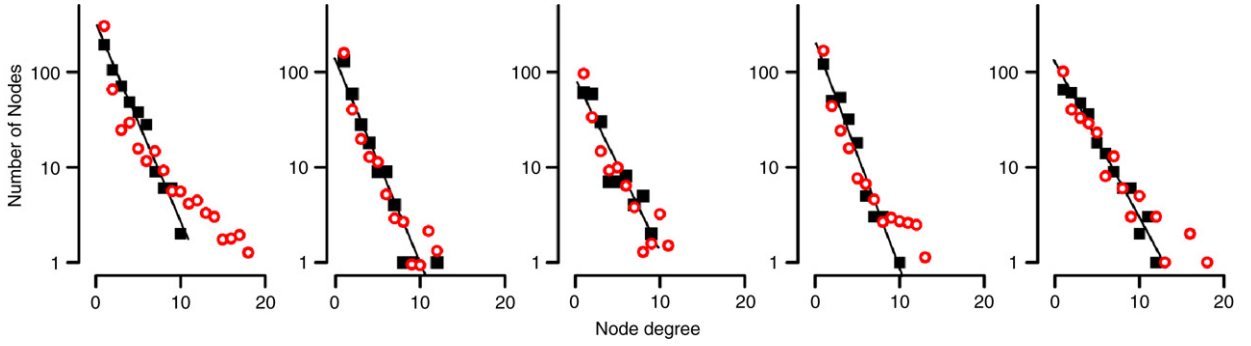


Fig. 4. Degree distribution for the gallery networks (black squares and exponential decay fit) and for networks obtained with an algorithm that greedily selects edges with higher betweenness centrality (open circles) (see text).

Moreover, social insects are capable of selecting shortest paths with similar feed-back mechanisms. For instance Goss et al. [41] have shown that Argentine ant *Linepithema humile* can select the shortest path to a food source. This phenomenon was modeled by Deneubourg et al. [42] as follows: let e^* be the edges incident to v and $e(t)$ be the number of insects that have used edge $e \in e^*$ after t time steps (this is assumed to be proportional to an amount of “pheromone marking” on the edge). The probability $P_e(t)$ for an insect to choose edge e at time $(t + 1)$ is

$$P_e(t) = \frac{(k + e(t))^n}{\sum_{\forall e \in e^*} (k + \tilde{e}(t))^n} \quad (7)$$

where the parameter n determines the degree of nonlinearity of the choice function: when n is large, if one branch has only slightly more pheromone than the other, the next ant that passes will have a high probability of choosing it. The parameter k quantifies the level of attraction of an unmarked branch.

In our simplification, we consider edge betweenness as an approximation for $e(t = 0)$. This has the advantage of relying on a classical network descriptor as edge betweenness [36]. We assume that the time scale \tilde{t} for removing an edge from the network is much longer than the passage time of insects $\tilde{t} \gg t$. Hence after a time span of \tilde{t} , the probability for an insect to pass across an edge will be close to zero if the edge had low betweenness ($P_e(\tilde{t}) \approx 0$ if $BC(e) = \min(BC(E))$) and the edge can be conveniently removed from the network.

Our algorithm, based on iterated computation of betweenness is very similar to the algorithm proposed by Newman and Girvan [43] to fragment a network into distinct communities. The main difference is that in Newman and Girvan [43] the edge with higher betweenness is removed at each step, while here we remove the edge with lower betweenness (without disconnecting the network).

The model we have proposed leads to networks with similar degree distribution to that of the gallery networks. Still, this model can yield networks that have proportionally more vertices with large degrees (see Fig. 4).

3.3. A multiobjective process with non optimal global transport performance

Gallery networks present significantly shorter average path lengths than the random spanning subgraphs (see Fig. 5). Still, none of the gallery networks is optimal for transportation efficiency. In particular, their performance is always worse than the one obtained with the maximum BC network (see Fig. 5).

This opens the question why the network of galleries is not an optimal spanning subgraph of the nest chambers. Several possibilities can be considered:

- (1) In the proposed maximum BC model used to generate low stretch spanning subgraphs, edges are progressively removed, starting from a G_M graph. In the real nests, edge removal seems to take place, and would be indicated by the high connectivity displayed by the nest under construction (M19). Still, it is unlikely that the starting graph is the maximally embedded network G_M .
- (2) The maximum BC model generates networks containing a few vertices with relatively high degree. It is likely that such highly connected vertices are physically impossible in termite constructions, because they would mine the architectural stability of the nest at a particular point. They could also concentrate too much traffic and become congested.
- (3) Termite activity is not uniformly distributed in these networks [25]. Some vertices will be associated with the presence of brood, others with the deposit of food, and the royal couple will be located at a particular point on the network. In addition, there are only very few entrance points to these networks, represented by chambers situated at the bottom of the nest. These vertices are quite peripheral when one considers displacements inside the nest, but they channel all the traffic from and to the nest.

In general, the paths between certain pairs of vertices will be more important than the other paths, and an optimal network will minimise distances along these paths, not the *average* distance among randomly chosen couples of vertices.

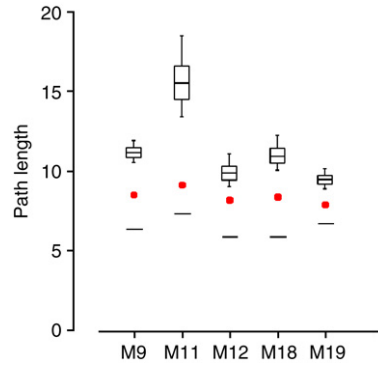


Fig. 5. Distribution of average topological path lengths in random spanning subgraphs (in black, $N = 10\,000$ and spanning subgraphs obtained with an algorithm that greedily retains edges with high betweenness (horizontal lines, see main text). The red circular dots indicate the performance of the real gallery network. All the graphs have the same average vertex degree (see text).

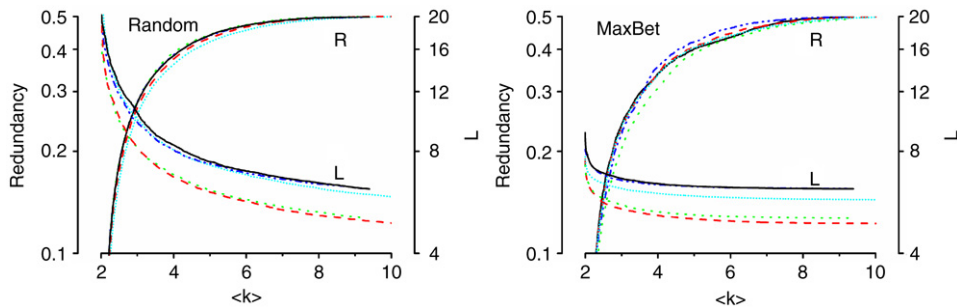


Fig. 6. Path length L and redundancy R are plotted against the average degree $\langle k \rangle$ for the two random network models. Left column: random spanning subgraphs; right column: maximum betweenness spanning subgraphs. Six curves are visible for both path length and redundancy in each plot; each curve is associated to subgraphs of the MEG of a different nest (M9: cyan short dot curve; M11: blue dash dot dot curve; M12 green dot curve; M18 red dash curve; M19 black solid curve). Networks with higher degree (in abscissa) have shorter values of L , but nearly maximal R , though maximum betweenness spanning subgraphs can somehow preserve low L even when they are relatively sparse. Optimisation of both L and R (both should be low) is likely to occur for values of $\langle k \rangle$ associated to regions of high steepness of the two curves.

More accurate models should include information about how individual vertices are used, but this information is not available for the dataset analysed here.

So far, we have compared the efficiency of the real gallery networks to the efficiency of random networks having the same total number of connections. However, termites could more simply reduce average path length by having more connected networks. The sparseness of *Cubitermes* networks despite that, suggests that there is a cost associated with increased number of edges.

These nests are important in protecting termites from attacks of predators, especially of ants. When part of the gallery network is attacked, termite defence consists in disconnecting the invaded chambers by closing the adjacent corridors with pellets of clay [44]. This actually corresponds to eliminating edges from the graph. The effect that the removal of a single edge plays on network topology is well quantified by our measure of local network redundancy R . In particular, when R is small, the disconnection of a single edge moves far away or disconnects network regions at the two ends of the edge. On the opposite, with large R , the removal of a single edge has smaller effects.

Unfortunately, the underlying generating model of real gallery networks is not known. This makes it difficult to know how average path length L and network redundancy R depend on the variable number of edges in the real gallery networks. Nevertheless, it is possible to investigate the relation between network degree $\langle k \rangle$, L and R in the two extreme network models. This relation is illustrated in Fig. 6, that plots L and R against $\langle k \rangle$ for the random spanning subgraph (left panel) and the maximum betweenness subgraph (right panel). Ideally, termites should minimise both parameters. However, L decreases rapidly when a few edges are added to the spanning tree, and then reaches a plateau for networks with average degree $\langle k \rangle \geq 4$ while R increases with similar progression for both the random and maximum betweenness network models. Accordingly, networks achieving a compromise between minimising both parameters will have an average degree falling in the steep part of both curves. This is actually observed in the real gallery networks, whose average degree is included in the interval $2.06 \leq \langle k \rangle \leq 3.27$.

4. Conclusions

Cubitermes networks of galleries are a particular class of real world 3D spatial networks.

In these networks, the set of possible connections is strongly limited by the fact that the elements represented by vertices fill all the space. This allows only connections to exist between physically adjacent vertices. Incidentally, the situation of space-filling interconnected elements is a very common feature of many biological systems and in particular of biological tissues, mostly due to the fact that they grow by intussusception (from inside) more than by apposition [45]. And it would be interesting to see if similar network structures are found for instance in the disposition of pores inside bones [46,47] and networks of cell to cell signalling (juxtacrine and paracrine [48]).

Termite networks of galleries are more efficient than random networks subject to similar spatial constraints. However, they do not reach optimal transportation efficiency. First, they are outperformed by networks having the same average degree and generated with a simple greedy algorithm to keep path length short. Second, they are extremely sparse, which in turn prevents fast communication between distant vertices to take place.

We argue that the sub optimal topological arrangement of connections reflects additional architectural or building constraints not considered by the model, for instance the impossibility of having vertices with very high degree. In addition, it is possible that these networks optimise paths between particular couples of vertices, not the average path length computed on all couples of vertices.

Network sparseness indicates that optimal transportation efficiency is not the only factor shaping the organisation of these networks. In particular, resilience to external attacks would be a key factor motivating for the low connectivity, given the particular defence strategy of *Cubitermes*.

In the future it will be interesting to see if some of the optimisation criteria proposed by different authors to model the topology of other transportation networks can also simulate this class of 3-D self-organised networks.

Acknowledgements

This work was supported by ANR-06-BYOS-0008 and by the CNRS interdisciplinary program “Complexité du Vivant”. A. Perna was supported during part of the project by a joint grant from the Ambassade de France in Rome and the Italian Ministero degli Affari Esteri.

References

- [1] S. Camazine, J.L. Deneubourg, N.R. Franks, J. Sneyd, G. Theraulaz, E. Bonabeau (Eds.), *Self-organization in Biological Systems*, Princeton University Press, Princeton, NJ, 2001 doi:10.1098/rsta.2003.1198.
- [2] S. Itzkovitz, U. Alon, *Phys. Rev. E* 71 (2005) 026117, doi:10.1103/PhysRevE.71.026117.
- [3] S. Boccaletti, V. Latora, Y. Moreno, M. Chavez, D.U. Hwang, *Phys. Rep. (Review Section of Physics Letters)* 424 (2006) 175, doi:10.1016/j.physrep.2005.10.009.
- [4] M. Rosvall, A. Trusina, P. Minnhagen, K. Sneppen, *Phys. Rev. Lett.* 94 (2005) 028701, doi:10.1103/PhysRevLett.94.028701.
- [5] P. Crucitti, V. Latora, S. Porta, *Phys. Rev. E* 73 (2006) 036125, doi:10.1103/PhysRevE.73.036125.
- [6] J. Buhl, J. Gautrais, N. Reeves, R.V. Sole, S. Valverde, P. Kuntz, G. Theraulaz, *Eur. Phys. J. B* 49 (2006) 513, doi:10.1140/epjb/e2006-00085-1.
- [7] A. Cardillo, S. Scellato, V. Latora, S. Porta, *Phys. Rev. E* 73 (2006) 066107, doi:10.1103/PhysRevE.73.066107.
- [8] S. Porta, P. Crucitti, V. Latora, *Physica A* 369 (2006) 853, doi:10.1016/j.physa.2005.12.063.
- [9] M.T. Gastner, M.E.J. Newman, *J. Stat. Mech.* (2006) P01015, doi:10.1088/1742-5468/2006/01/P01015.
- [10] A. Barrat, M. Barthelemy, R. Pastor-Satorras, A. Vespignani, *PNAS* 101 (2004) 3747, doi:10.1073/pnas.0400087101.
- [11] R. Guimera, S. Mossa, A. Turttschi, L.A.N. Amaral, *PNAS* 102 (2005) 7794, doi:10.1073/pnas.0407994102.
- [12] A. Barrat, M. Barthelemy, A. Vespignani, *J. Stat. Mech.* (2005) P05003, doi:10.1088/1742-5468/2005/05/P05003.
- [13] J.R. Banavar, A. Maritan, A. Rinaldo, *Nature* 399 (1999) 130, doi:10.1038/20144.
- [14] M. Durand, *Phys. Rev. Lett.* 98 (2007) 088701, doi:10.1103/PhysRevLett.98.088701.
- [15] V. Colizza, J.R. Banavar, A. Maritan, A. Rinaldo, *Phys. Rev. Lett.* 92 (2004) 198701, doi:10.1103/PhysRevLett.92.198701.
- [16] M.T. Gastner, M.E.J. Newman, *Eur. Phys. J. B* 49 (2006) 247, doi:10.1140/epjb/e2006-00046-8.
- [17] M. Barthelemy, A. Flammini, *J. Stat. Mech.* (2006) L07002, doi:10.1088/1742-5468/2006/07/L07002.
- [18] M. Barthelemy, A. Flammini, Preprint. <http://www.citebase.org/abstract?id=oai:arXiv.org:0708.4360>.
- [19] F. Papi, *Animal Homing*, Chapman & Hall, London, 1992.
- [20] D.E. Jackson, M. Holcombe, F.L.W. Ratnieks, *Nature* 432 (2004) 907, doi:10.1038/nature03105.
- [21] D. Cherix, *Insectes Soc.* 27 (1980) 226.
- [22] P. Jmhasly, R.H. Leuthold, *Insectes Soc.* 46 (1999) 332.
- [23] J. Buhl, J. Gautrais, R.V. Solé, P. Kuntz, S. Valverde, J.L. Deneubourg, G. Theraulaz, *Eur. Phys. J. B* 42 (2004) 123, doi:10.1140/epjb/e2004-00364-9.
- [24] J. Desneux, *Insectes Soc.* 3 (1956) 277.
- [25] P.P. Grassé, *Termitologie*, tome 2: Fondation des sociétés, Construction, Masson, Paris, 1984.
- [26] M. Lüscher, *Acta Trop* 12 (1955) 289.
- [27] J.S. Turner, *J. Arid Environ.* 28 (1994) 231.
- [28] J. Korb, K. Linsenmair, *Behav. Ecol.* 10 (1999) 312.
- [29] J. Korb, K. Linsenmair, *Behav. Ecol.* 11 (2000) 486.
- [30] J.S. Turner, *The Extended Organism: The Physiology of Animal-built Structures*, Harvard University Press, 2000.
- [31] J.S. Turner, *Physiol. Biochem. Zoology* 74 (2001) 798, doi:10.1086/323990.
- [32] J. Korb, *Naturwissenschaften* 90 (2003) 212.
- [33] C. Noirot, C. Noirot-Timothee, *Sympos. Genet. Biol. Italica* 11 (1962) 180.
- [34] A. Perna, C. Jost, E. Couturier, S. Valverde, S. Douady, G. Theraulaz, *Naturwissenschaften* xx (2008) xxx, doi:10.1007/s00114-008-0388-6.
- [35] Somatom Sensation16; Siemens, Erlangen, Germany, using exposure parameters of 120 kV and 150 mAs slice thickness of 1 mm, interslice distance 0.5 mm.
- [36] J.M. Anthonisse, Technical Report, Stichting mathematisch centrum, Amsterdam, 1971.

- [37] D.J. Watts, *Small Worlds: The Dynamics of Networks between Order and Randomness*, Princeton University Press, Princeton, 1999.
- [38] A.E. Motter, T. Nishikawa, Y. Lai, *Phys. Rev. E* 66 (2002) 065103, doi:10.1103/PhysRevE.66.065103.
- [39] J.G. Propp, D.B. Wilson, *J. Algorithms* 27 (1998) 170.
- [40] S. Scellato, A. Cardillo, V. Latora, S. Porta, *Eur. Phys. J. B* 50 (2006) 221, doi:10.1103/PhysRevE.73.066107.
- [41] S. Goss, S. Aron, J.L. Deneubourg, J.M. Pasteels, *Naturwissenschaften* 76 (1989) 579, doi:10.1007/BF00462870.
- [42] J.L. Deneubourg, S. Aron, S. Goss, J.M. Pasteels, *J. Insect Behav.* 3 (1990) 159.
- [43] M.E.J. Newman, M. Girvan, Finding and evaluating community structure in networks, *Phys. Rev. E* 69 (2004) 026113, doi:10.1103/PhysRevE.69.026113.
- [44] A. Dejean, R. Fénéron, *Behav. Processes* 47 (1999) 125.
- [45] D'Arcy Wentworth Thompson, *On Growth and Form: The Complete Revised Edition*, Dover, 1992.
- [46] L.D.F. Costa, M.P. Viana, M.E. Beletti, *Appl. Phys. Lett.* 88 (2006) 033903, doi:10.1063/1.2166473.
- [47] J.R. Jones, G. Poologasundarampillai, R.C. Atwood, D. Bernard, P.D. Lee, *Biomaterials* 28 (2007) 1404, doi:10.1016/j.biomaterials.2006.11.014.
- [48] B. Alberts, A. Johnson, J. Lewis, M. Raff, K. Roberts, P. Walter, *Molecular biology of the cell*, Garland Sci. 5 (2007).